Electronic Supplementary Information (ESI)

A Three Dimensional (Time, Wavelength and Intensity) Functioning Fluorescent Probe for the Selective Recognition/Discrimination of Cu^{2+}, Hg^{2+}, Fe^{3+} and F^- ions

Qin Ruan,[a] Lan Mu,[a] Xi Zeng,*[a] Jiang-Lin Zhao,*[b] Li Zeng,[a] Zhen-Min Chen,[b] Cai Yang,[b] Gang Wei*[c] and Carl Redshaw[d]

[a] *Key Laboratory of Macrocyclic and Supramolecular Chemistry of Guizhou Province; School of Chemistry and Chemical engineering, Guizhou University, Guiyang 550025, China. E-mail: zengxi1962@163.com*

[b] *Shenzhen Institutes of Advanced Technology, Chinese Academy of Sciences, 1068 Xueyuan Avenue, Shenzhen 518055, China. E-mail: zhaojianglin1314@163.com*

[c] *CSIRO Manufacturing, PO Box 218, NSW 2070, Australia. E-mail: gang.wei@csiro.au*

[d] *Chemistry, School of Mathematics and Physical Sciences, University of Hull, Hull HU6 7RX, U.K.*

1. Materials and Methods

Unless otherwise stated, all reagents used were purchased from commercial sources and were used without further purification. The solutions of the metal ions were prepared from their perchlorate salts (Aldrich and Alfa Aesar Chemical Co., Ltd.). All the anions used were tetra-*n*-butylammonium salts (Sigma-Aldrich Chemical Co., Ltd.), and were stored in a desiccator under vacuum containing self-indicating silica. Double distilled water was used throughout. Fluorescence spectral measurements were performed on a Cary Eclipse fluorescence spectrophotometer (Agilent Technologies) equipped with a xenon discharge lamp using a 1 cm quartz cell. UV-Vis absorption spectra were conducted on a UV-1800 spectrophotometer (Shimadzu) in a 1 cm quartz cell. IR spectra were obtained using a Vertex 70 FT-IR spectrometer (Bruker). ^{1}H and ^{13}C NMR spectra were measured on JEOL JNM-ECZ400S 400 MHz NMR spectrometer (JEOL) and WNMR-I 500 MHz NMR spectrometer respectively at room temperature using TMS as an internal standard. MALDI-TOF mass spectra were measured on a AB SCIEX TripleTOF$^{AM\ 5600}$ System. Microelectrode layers using the sputtering and lift-off process with the standard photo-lithography (EVG 610, Austria). Cell fluorescence imaging was performed using a Ti (Nikon) fluorescent inverted phase contrast microscope.

Spectral measurement

To a 10 mL volumetric flask containing different amounts of ions, the appropriate amounts of the solution of probe **L** were added using a micropipette. For Hg^{2+}, $Fe^{3+}$and Cu^{2+}, the system was then diluted with CH_3CN/H_2O (97/3, v/v, pH = 7) mixed solvent to 10 mL; for F^-, it was diluted with CH_3CN to 10 mL, and then the fluorescence sensing of the ions was conducted. The fluorescence spectra were measured after addition of the ions at room temperature and when equilibrium was reached. Fluorescence measurements were carried out with an excitation and emission slit width of 10 nm.

Cell culture and fluorescence imaging

PC3 cells were grown using a Roswell Park Memorial Institute Medium Modified supplemented with 10% fetal bovine serum, 100 U/mL penicillin and 100 μg/mL streptomycin at 37 °C and 5% CO_2. One day prior to imaging, the cells were seeded in 6-well flat-bottomed plates. The next day, the cells were incubated with 10 μM of probe **L** for 50 min at 37 °C. Before incubating with 50

μM Hg^{2+}, Fe^{3+} or Cu^{2+} for another 40 ~ 50 min, the cells were rinsed with fresh culture medium three times to remove the remaining sensor, then the fluorescence imaging of intracellular Hg^{2+}, Fe^{3+} and Cu^{2+} was observed under an inverted fluorescence microscope.

Determination of cytotoxicity by MTT assay

Cell viability was determined by using MTT (3-(4,5-dimethylthiazol-2-yl)-2,5-diphenyltetrazolium bromide) assays (Sigma-Aldrich). Living cells were plated in a 96-well plate at a concentration of 1×10^5 cells per well. The cells were treated with different concentrations of probe **L** (0, 10, 50, 100 and 500μM) for about 60 min in a humidified incubator at 37 °C, 5% CO_2. 20μL MTT solution was added to each well of the plate, followed by incubation at 37 °C for 4 h. The supernatants were then aspirated carefully, and the formazan product was dissolved with 150 μL dimethyl sulfoxide. The absorbance was measured at a wavelength of 630 nm with a microplate reader (Multiskan GO，Thermo, USA).

2. Synthesis and Characterization of probe L

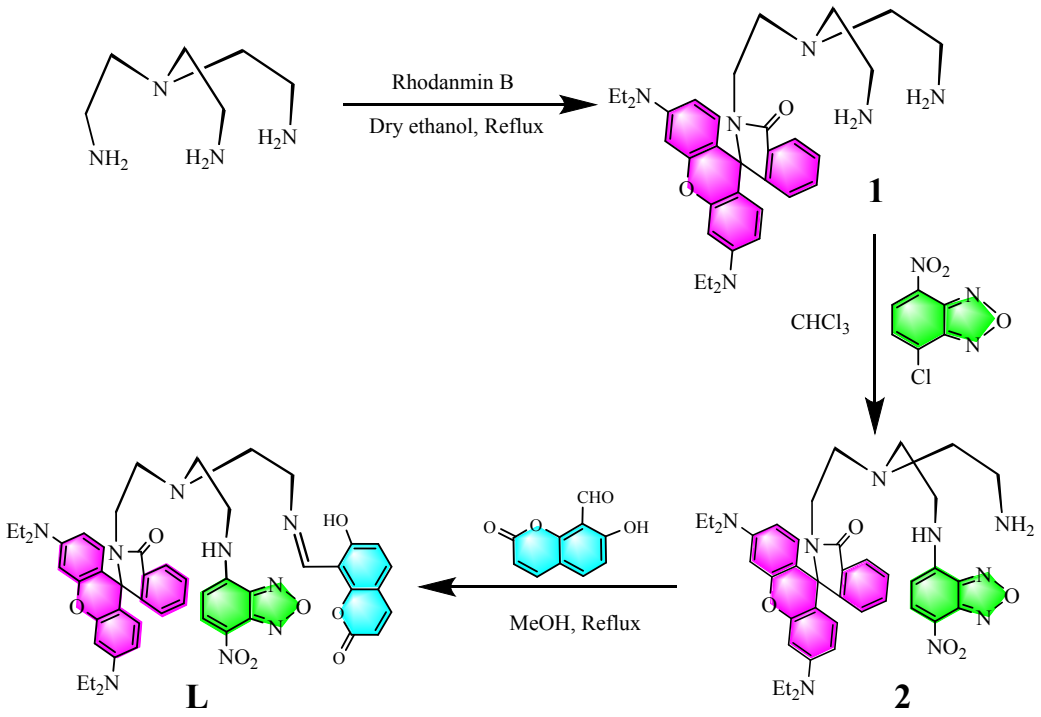

Scheme S1. The synthesis of fluorescent probe **L**.

Compounds **1** and **2** were prepared following the reported procedures.[1] Typically, a

mixture of tris(2-aminoethyl)amine (4.0 g, 27.36 mmol) and Rhodamine B (1.638 g, 3.42 mmol) in dry ethanol (60 mL) was refluxed for 24 h under an N_2 atmosphere. The solvent was then removed by evaporation, and the residue was extracted with CH_2Cl_2 (100 mL) three times, washed with water and dried with $MgSO_4$ overnight. The CH_2Cl_2 solvent was removed by evaporation to afford a light red oily product. The crude product was purified by column chromatography ($MeOH/CHCl_3/NEt_3$ = 9/1/1, v/v) to afford 1.71g of a colourless oil **1** in 87.3% yield.

To a stirring solution of **1** (0.6 g, 0.8 mmol) in toluene (30 mL), Et_3N (0.5 mL, 5 mmol) was added followed by NBD-Cl (0.16 g, 0.8 mmol) and the system was stirred for 8 h under reflux. On cooling, the solution was filtered and evaporated to dryness under reduced pressure. Water was added to the residual mass, which was extracted with $CHCl_3$ (3 × 50 mL). The combined organic layers, after drying over anhydrous Na_2SO_4 were evaporated under reduced pressure. The desired compound **2** was obtained as a reddish coloured solid after further isolation and purification by passing through a column of silica in 1% MeOH in $CHCl_3$ as an eluent.

Finally, a mixture of intermediate **2** (500 mg, 0.68 mmol) and 7-hydroxy-2-oxo-*2H*-chromene-8-carbaldehyde (110 mg, 0.748mmol) in dry MeOH (60 mL) was refluxed for 8 h under N_2 atmosphere. The solvent was removed by evaporation, and then the crude product was purified by column chromatography ($CHCl_3$/MeOH = 100/2, v/v) to give 260 mg of an orange solid **L** in 42.6% yield. m.p. 147 ~149 °C; ^{1}H NMR (500 M, DMSO-d^6, ppm) δ: 14.01 (s, 1 H, -O*H*), 9.07 (s, 1 H, -C*H*=N), 8.57 (s,1 H, -C-NH), 8.32 (d, *J* = 5 Hz ,1 H, Ar-H), 7.79 (d, *J* = 10 Hz, 1 H, Ar-H), 7.72 (d, *J* = 10 Hz, 1 H, Ar-H), 7.52 (br, 2 H, Ar-H × 2), 7.26 (d, *J* = 10 Hz, 1 H, Ar-H), 7.06 (d, *J* = 5 Hz, 1 H, Ar-H), 6.34 (m, 5 H, Ar-H), 6.14 (d, *J* = 10 Hz, 2 H, Ar-H), 6.09 (d, *J* = 10 Hz, 1 H, Ar-H), 6.0 (d, *J* = 5Hz, 1 H, Ar-H), 3.27 ~ 3.26 (m, 8 H, N*CH*$_2$CH$_3$×4), 3.11 (br, 2 H, NCH_2CH_2N), 2.66 ~ 2.62 (m, 4 H, NCH_2CH_2N), 2.36~ 2.30 (m, 2 H, NCH_2CH_2N), 2.08 (bs, 4H, NCH_2CH_2N) and 1.03-1.01 (m, 12 H, NCH_2CH_3); ^{13}C NMR (125 M, DMSO-d^6, ppm) δ: 206.63, 190.41, 176.00, 166.48, 159.65, 159.29, 156.18, 152.74, 148.29, 145.12, 145.02, 144.00, 143.67, 137.50, 133.45, 132.60, 130.81, 128.47, 128.30, 123.57, 122.22, 120.39, 119.15, 108.09, 107.48, 104.99, 104.76, 102.88, 98.85, 96.97, 79.04, 64.07, 52.00, 51.37, 45.62, 43.53, 41.30, 36.83, 30.60, 12.20; MS (ESI/TOF-Q) Calcd for $[C_{50}H_{52}N_9O_8]$: m/z 906.39388, Found: m/z 906.39436 $[M+H]^+$.

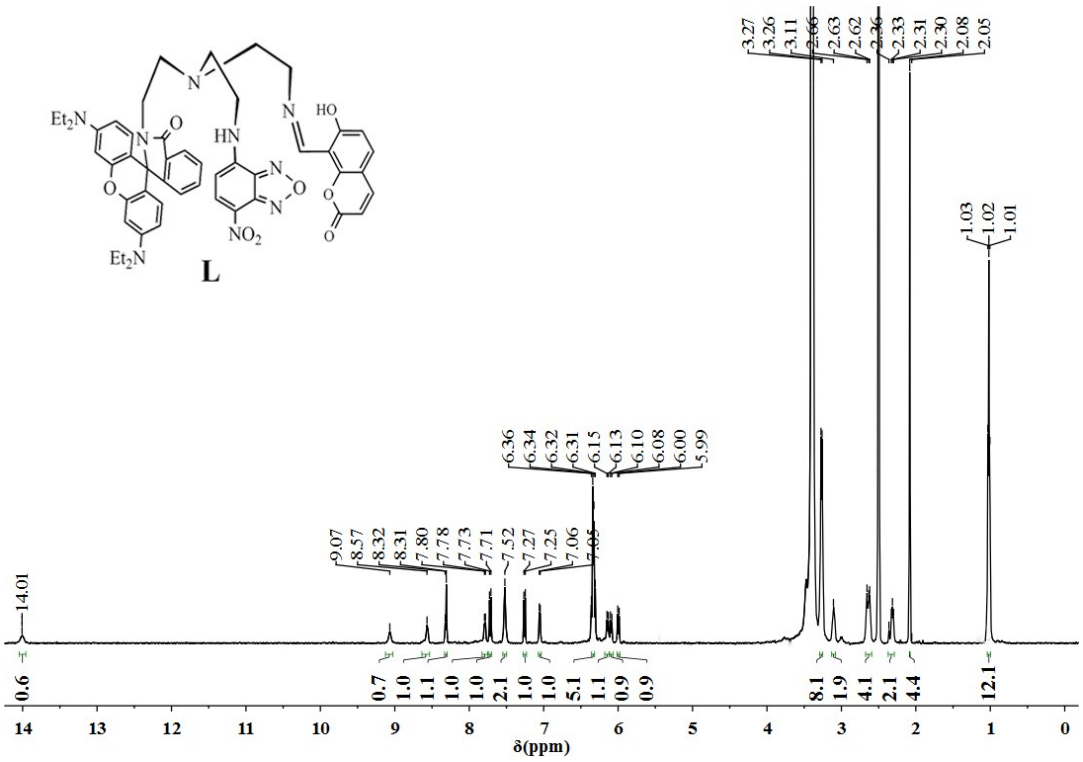

Figure S1. ^{1}H NMR spectrum of probe **L** in DMSO-d^6 at 25 °C at 500 MHz.

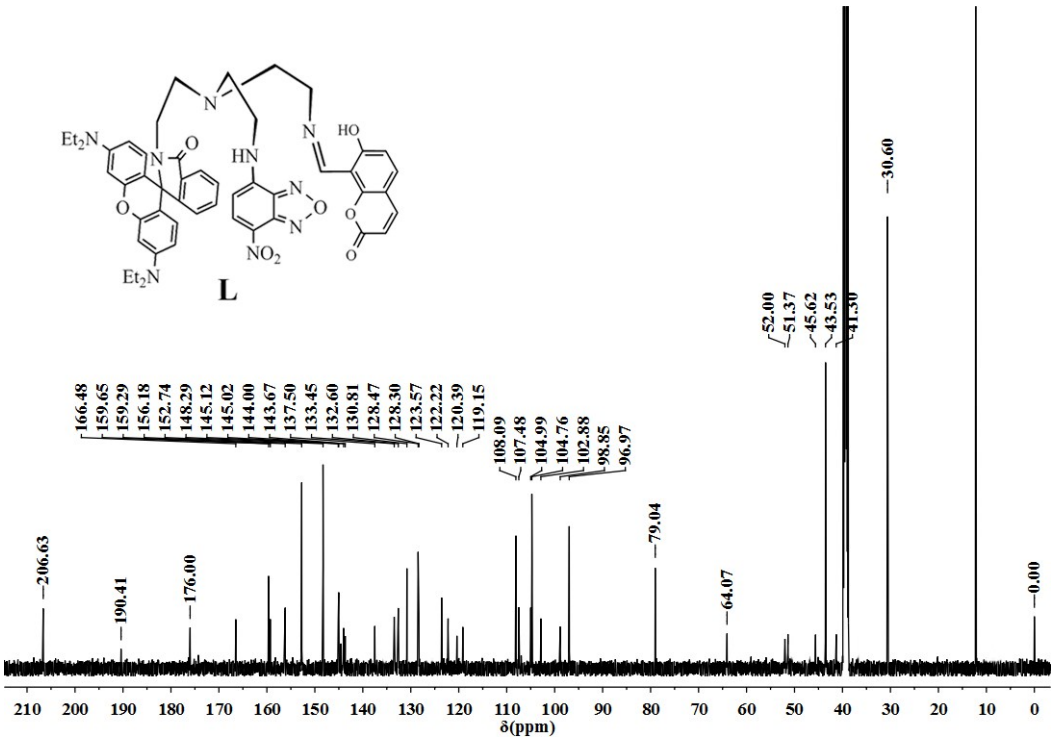

Figure S2. ^{13}C NMR spectrum of probe **L** in DMSO-d^6 at 25 °C (125 MHz).

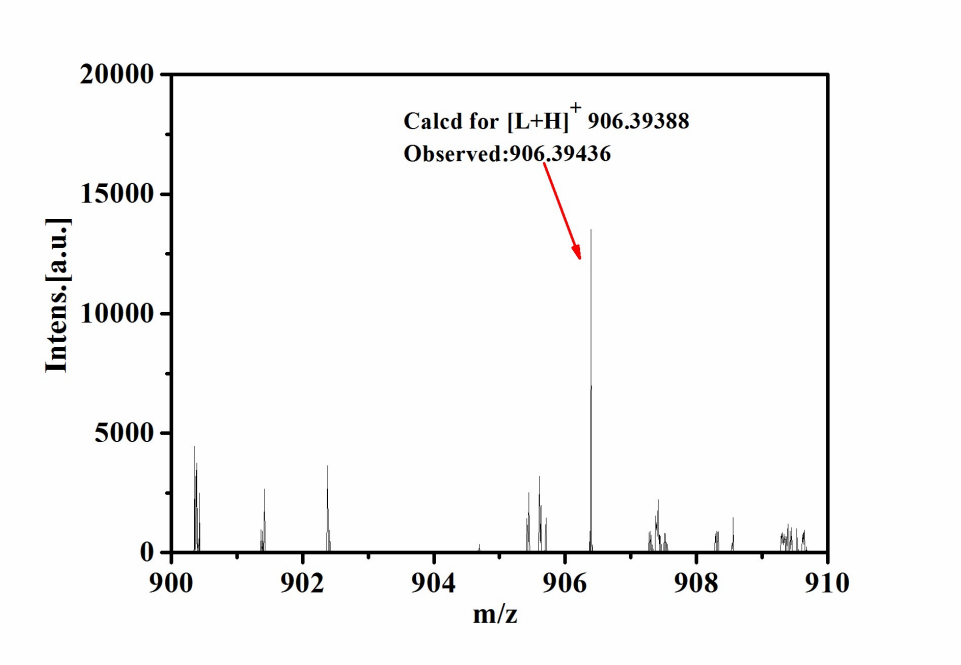

Figure S3. Mass spectrum of probe **L**.

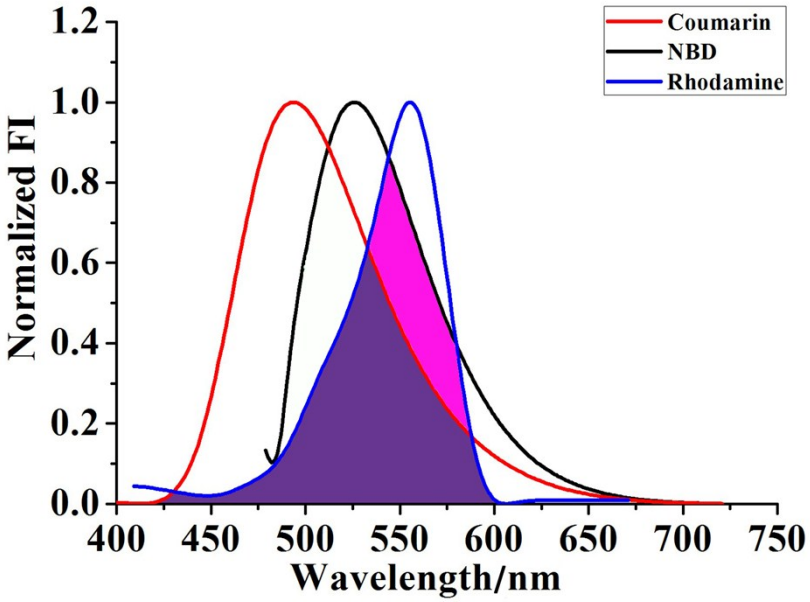

Figure S4. Spectral overlap between the energy donor coumarin, 7-nitrobenz-2-oxa-1,3-diazole (NBD) and acceptor rhodamine absorption. $\lambda_{ex\ (Coumarin)}$ = 365 nm and $\lambda_{ex\ (NBD)}$ = 470 nm.

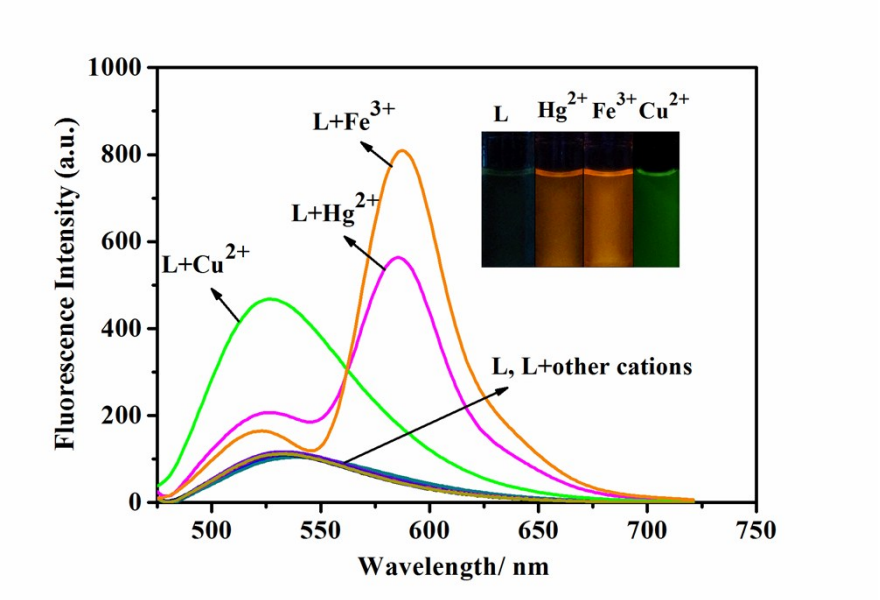

Figure S5. Fluorescence spectrum of probe **L** (20 μM) with 20 equiv. of different metal ions (measured after 100 min, λ_{ex} = 470 nm) in CH_3CN/H_2O (97/3, v/v, Tris-HCl, pH 7) solution (inset shows the colour change of probe **L** in the absence and the presence of Hg^{2+}, Cu^{2+} and Fe^{3+} under UV-vis light.).

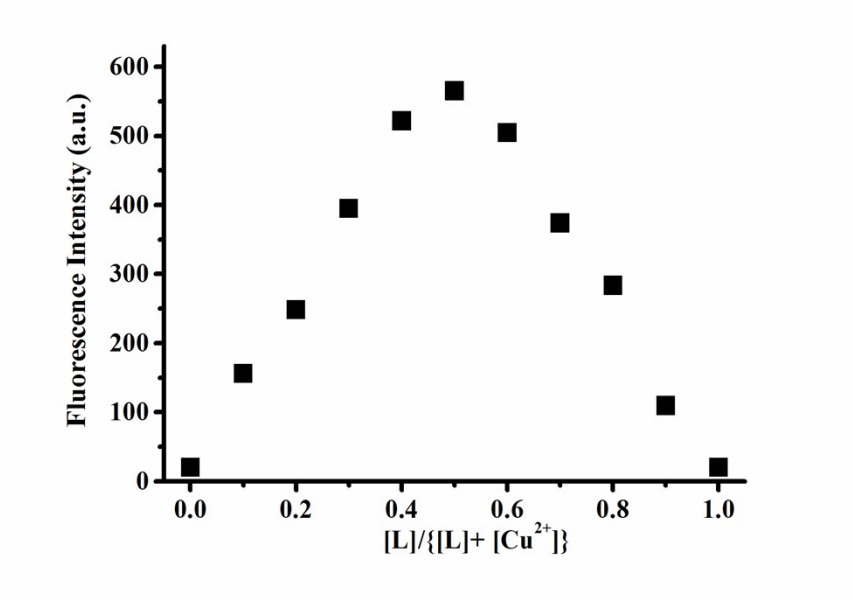

Figure S6. The Job's plot data of probe **L** with Cu^{2+}.

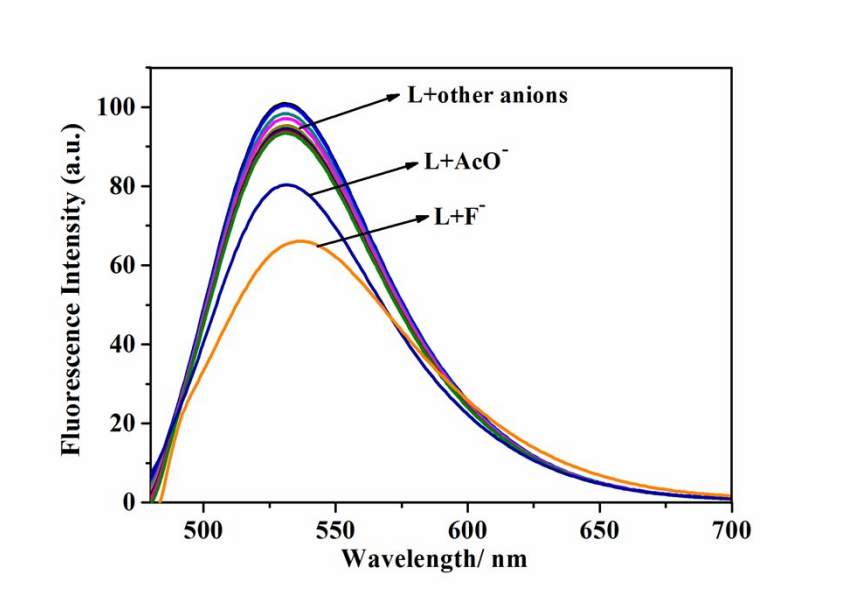

Figure S7. Fluorescence spectrum of probe **L** (20 μM) with 10 equiv. different anions (F^-, Cl^-, Br^-, I^-, NO^{3-}, HSO_4^-, $H_2PO_4^-$, ClO_4^- and AcO^-) in CH_3CN solution; λ_{ex}/ λ_{em} = 470 nm/525 nm.

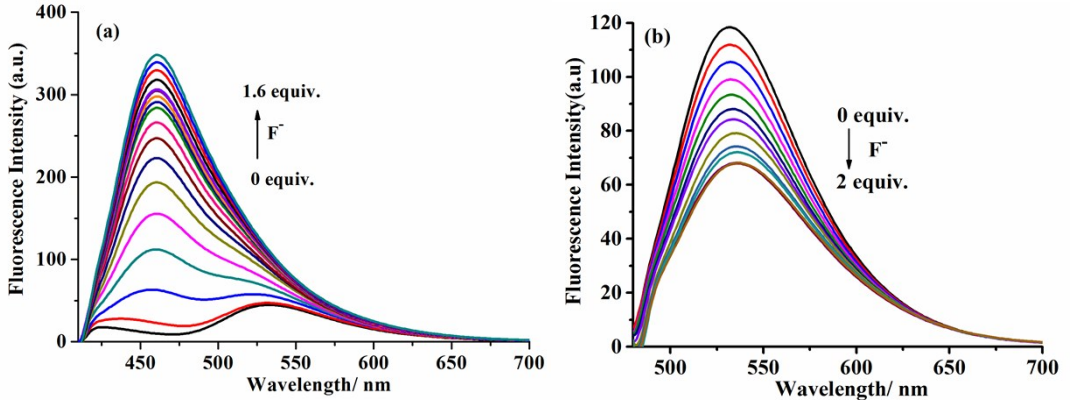

Figure S8. Fluorescence spectral titration of probe **L** (20 μM) with F^- in CH_3CN solution; (a) λ_{ex}/ λ_{em} = 365 nm/460 nm; (b) λ_{ex}/ λ_{em} = 470 nm/525 nm.

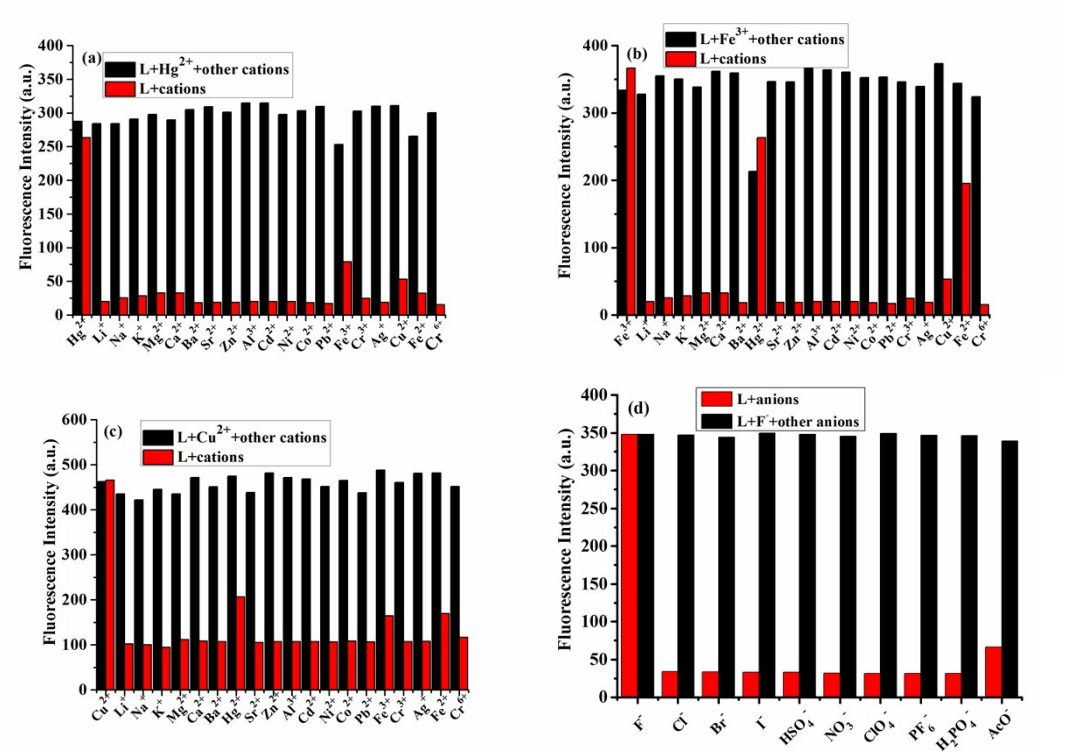

Figure S9. Fluorescence response of probe **L** (20 μM). Red bars: emission intensity of probe **L** on addition of the respective ions (20 equiv.). Black bars: emission intensity of probe **L** on addition of the respective competing ions (20 equiv.); (a) λ_{ex}/ λ_{em} = 365 nm/585 nm, (CH_3CN/H_2O, 97/3, v/v, Tris-HCl, pH 7), measured after 2 min; (b) λ_{ex}/ λ_{em} = 365 nm/585 nm, (CH_3CN/H_2O, 97/3, v/v, Tris-HCl, pH 7), measured after 100 min; (c) λ_{ex}/ λ_{em} = 470 nm/525 nm, (CH_3CN/H_2O, 97/3, v/v, Tris-HCl, pH 7), measured after 100 min and (d) λ_{ex}/ λ_{em} = 365 nm/460 nm, (CH_3CN), measured after 2 min.

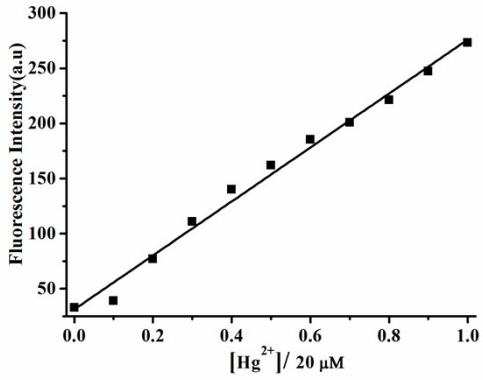

Figure S10. Fluorescence intensity calibration curve of probe **L** (20 μM) as a function of Hg^{2+} (measured immediately) concentration in CH_3CN/H_2O (97/3, v/v, Tris-HCl, pH 7) solution; λ_{ex}/ λ_{em} = 360 nm/ 585 nm; Y = 244.7 X + 31.26, R^2= 0.9893, (n = 11), 2 ~ 20 μM, LOD = 0.110 μM.

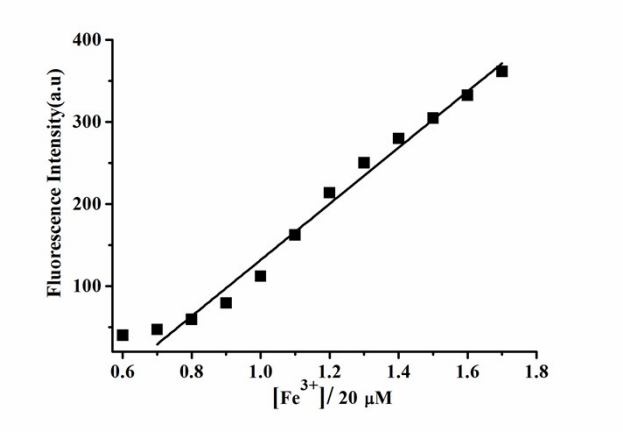

Figure S11. Fluorescence intensity calibration curve of probe **L** (20 μM) as a function of Fe^{3+} (measured after 1.5 h) concentration in CH_3CN/H_2O (97/3, v/v, Tris-HCl, pH 7) solution; $\lambda_{ex}/\ \lambda_{em}$ = 365 nm/ 585 nm; Y = -210.6 + 342.4 X, R^2 = 0.9851, (n = 12), 12 ~ 36 μM LOD = 0.074 μM.

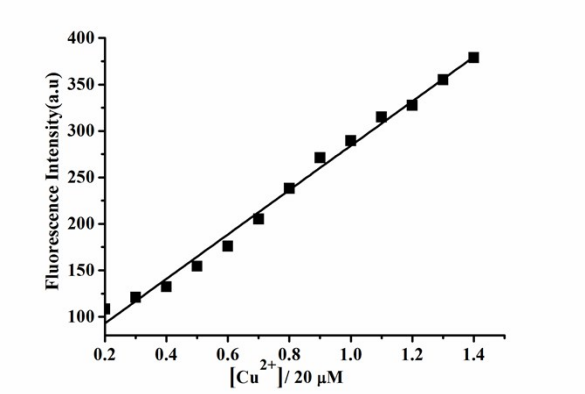

Figure S12. Fluorescence intensity calibration curve of probe **L** (20 μM) as a function of Cu^{2+} concentration in CH_3CN/H_2O (97/3, v/v, Tris-HCl, pH 7) solution; $\lambda_{ex}/\ \lambda_{em}$ = 470 nm/ 525 nm; Y = 45.19 + 239.0 X, R^2 = 0.9910, (n = 13), 4 ~ 28 μM, LOD = 0.110 μM.

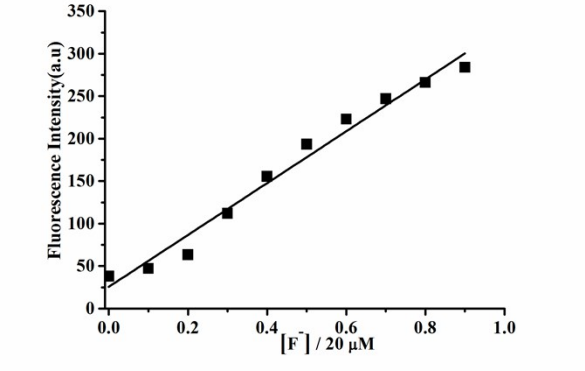

Figure S13. Fluorescence intensity calibration curve of probe **L** (20 μM) as a function of F^- concentration in CH_3CN; $\lambda_{ex}/\ \lambda_{em}$ = 365 nm/ 460 nm; Y = 25.69 X + 305.1, R = 0.9764 (n = 10), 2~ 20 μM LOD = 0.106 μM.

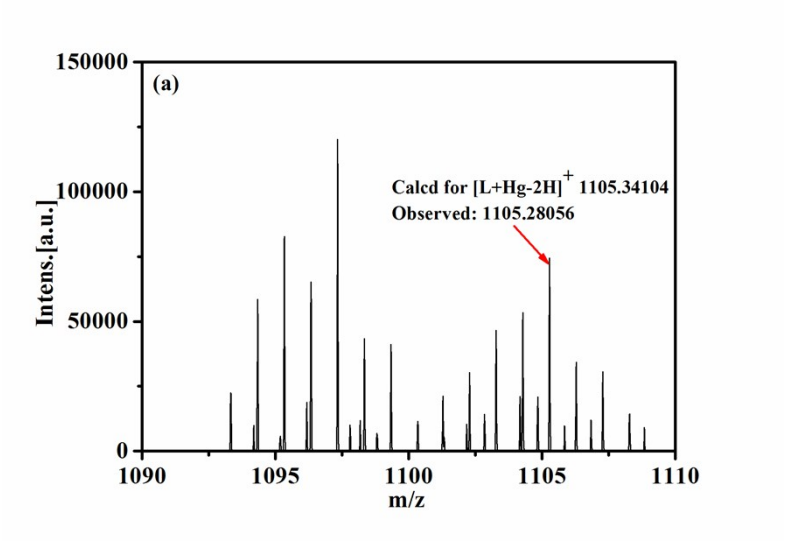

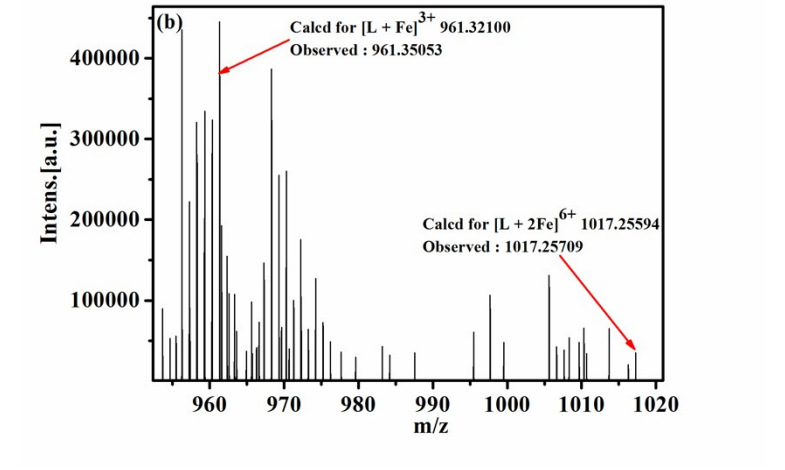

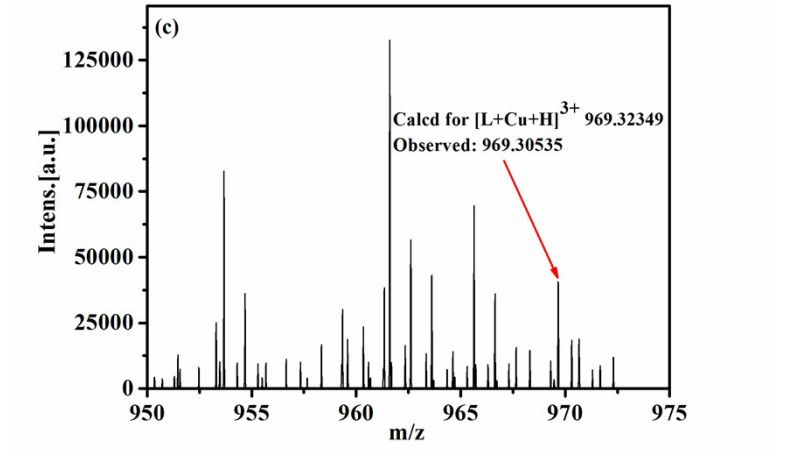

Figure S14. (a) Mass spectrum of probe **L** with Hg^{2+}; (b) Mass spectrum of probe **L** with Fe^{3+}; (c) Mass spectrum of probe **L** with Cu^{2+}.

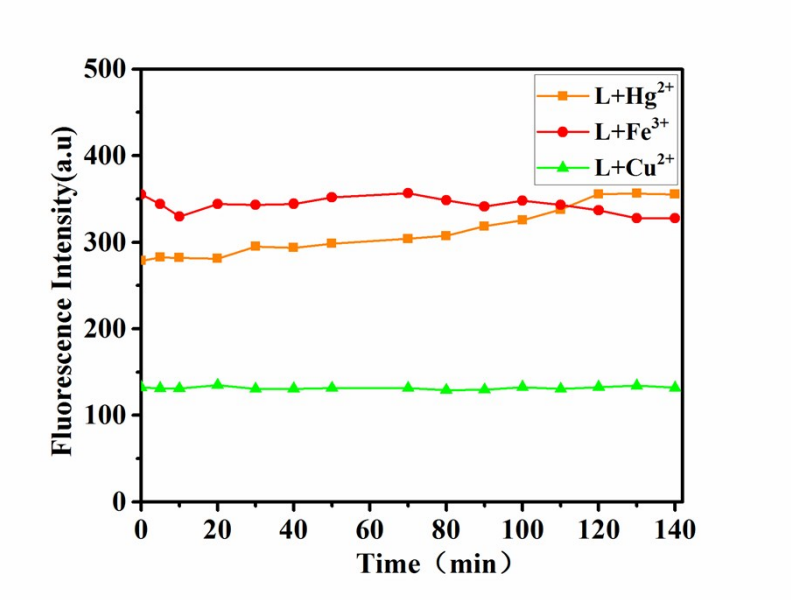

Figure S15. Effect of time on fluorescence intensity of the probe **L** with 20 equiv. of different metal ions (measured after equilibrium) in CH_3CN/H_2O (97/3, v/v, Tris-HCl, pH 7) solution. Hg^{2+} (λ_{ex}/ λ_{em} = 365 nm/585 nm), Fe^{3+} (λ_{ex}/ λ_{em} = 365nm/ 585 nm) and Cu^{2+} (λ_{ex}/ λ_{em} = 365 nm/ 525 nm).

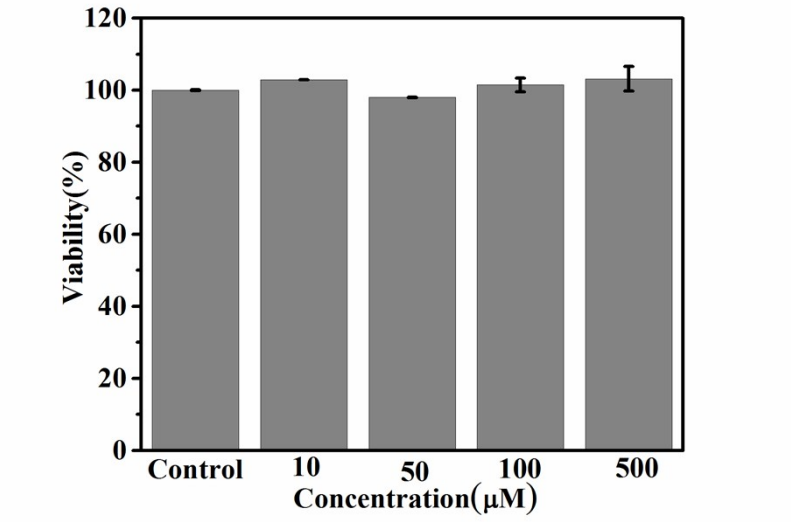

Figure S16. Assessment of cytotoxicity of different concentrations of probe **L** for 1 h living cells using the cytotoxicity assay (MTT assay). It was performed by directly determining the effect of probe **L** on cellular viability of living cell under our laboratory conditions. The living cell was either treated with different concentrations of probe **L** (10, 50, 100 and 500μM) or left untreated as a control. The results showed that probe **L** at the concentrations 0, 10, 50, 100 and 500μM had no significant effect on cell viability over about 60 min.

Table S1. Analysis parameters for probe **L** and detection of Hg^{2+}, Fe^{3+}, Cu^{2+} and F^-.

Ion	The linear range of the calibration curve [μM]	Correlation coefficient	Limits of detection [μM][a]	Association constants K_a [M^{-1}][b] (±% K_{error}[c])
Hg^{2+} (λ_{ex}/ λ_{em} = 365/ 585 nm)	2 ~ 20	0.9893	0.110	1.787×10^{13} (±288751)
Fe^{3+} (λ_{ex} / λ_{em} = 365/ 585 nm)	12 ~ 36	0.9851	0.074	K_1=1.739×10^4 (±2) K_2=4.887×10^3 (±22)
Cu^{2+} (λ_{ex} / λ_{em} = 470/ 525 nm)	4 ~ 28	0.9910	0.110	1.347×10^5 (±332)
F^- (λ_{ex} / λ_{em} = 365/ 460 nm)	2 ~ 20	0.9764	0.106	9.196×10^5 (±352)

[a] The limits of detection (LOD) of probe **L** were determined using the following equation: LOD = 3δ/*K*, δ is the standard deviation of the blank solution and *K* is the slope of the calibration curve. [b] Association constants (K_a) based on the fluorescent titration data were calculated using the Thordarson's global-fit method.[2] [c] The % error here is not a measure of precision of replicates but represents the % error resulting from the global-fit calculations since only single titration experiments in each case were conducted.

Table S2. Recovery assay of spiked of ions in tap water

Sample	Ion	The addition of ion (μM)	Detected (mean ± SD, μM)	Recovery rate (%)	R.S.D. (% n=3)
Tap Water samples *	Hg^+	0	-	-	-
		8.00	7.50	93.75	1.52
		12.00	12.95	107.92	3.92
		16.00	16.88	105.48	2.21
	Fe^{3+}	0	-	-	-
		14.00	14.06	100.42	0.36
		24.00	24.02	100.06	1.27
		34.00	33.45	98.39	1.54
	Cu^{2+}	0	-	-	-
		8.00	7.54	94.27	2.94
		12.00	13.04	108.58	4.10
		16.00	15.98	99.85	0.66

* Derived from Guizhou university laboratory tap water.

Reference:

1. (*a*) Z. Li, J.-L. Zhao, Y.-T. Wu, L. Mu, X. Zeng, Z. Jin, G. Wei, N. Xie and C. Redshaw, *Org. Biomol. Chem.*, 2017, **15**, 8627–8633; (*b*) B. Biswal, A. Pal and B. Bag, *Dalton Trans.*, 2017, **46**, 8975–8991.
2. (*a*) P. Thordarson, *Chem. Soc. Rev.*, 2011, **40**, 1305–1323; (b) http://supramolecular.org; (c) P. Job, *Ann. Chim.*, 1928, **9**, 113–203.